

## Load transfer and deformation mechanisms in carbon nanotube-polystyrene composites

D. Qian and E. C. Dickey<sup>a)</sup>

*Department of Chemical and Materials Engineering, University of Kentucky, Lexington, Kentucky 40506*

R. Andrews and T. Rantell

*Center for Applied Energy Research, University of Kentucky, Lexington, Kentucky 40511*

(Received 12 January 2000; accepted for publication 21 March 2000)

Multiwall carbon nanotubes have been dispersed homogeneously throughout polystyrene matrices by a simple solution-evaporation method without destroying the integrity of the nanotubes. Tensile tests on composite films show that 1 wt % nanotube additions result in 36%–42% and ~25% increases in elastic modulus and break stress, respectively, indicating significant load transfer across the nanotube-matrix interface. *In situ* transmission electron microscopy studies provided information regarding composite deformation mechanisms and interfacial bonding between the multiwall nanotubes and polymer matrix. © 2000 American Institute of Physics. [S0003-6951(00)04120-6]

Carbon nanotubes (NTs) have many remarkable physical characteristics such as novel electronic properties,<sup>1</sup> exceptionally high axial strengths and axial Young's moduli of the order of terra pascal.<sup>2–4</sup> The exact magnitude of these properties depends on the diameter and chirality of the NT and whether they are in single-wall or multiwall form. Because of their outstanding physical properties, carbon nanotubes have numerous potential applications.<sup>5</sup> One class of nanotube materials is NT composites in which the nanotube architecture is established within a host matrix material. Foreseeable NT-polymer composite materials include those designed for structural applications or for functional applications that make use of their conductivity, electromagnetic interference shielding<sup>6,7</sup> and optoelectronic properties.<sup>8</sup> Large-scale production of NT composites will, of course, depend upon a large and inexpensive supply of high quality nanotubes. Several continuous chemical vapor deposition methods may hopefully meet this requirement in the near future.<sup>9,10</sup>

The effective utilization of nanotubes in composite applications depends strongly on the ability to disperse the NTs homogeneously throughout the matrix without destroying the integrity of the NTs. Furthermore, good interfacial bonding is required to achieve load transfer across the NT-matrix interface, a necessary condition for improving the mechanical properties of polymer composites. Polymer-NT composites have been the topic of several recent studies which used epoxy resins<sup>6,11–15</sup> and thermoplastic polymers<sup>16,17</sup> as the matrix materials. In these studies the important issue of NT dispersion was not, however, studied in great detail. In this letter, we address both nanotube dispersion and deformation mechanisms in polymer composites by studying a model composite system in which multiwall NTs (MWNTs) are dispersed in a polystyrene (PS) matrix. The homogeneity of the composites and deformation mechanisms are studied by

*in situ* transmission electron microscopy (TEM).

In this work we employed a simple solution-evaporation<sup>18</sup> method assisted by high-energy sonication to prepare uniform MWNT-PS composite samples. First, the PS (48 000 or 280 000 molecular weight from Aldrich Chemical Company, Inc.) was dissolved in toluene with a mass ratio of 1:10. The MWNTs were dispersed separately in toluene by high-energy sonication using an ultrasonic wand dismembrator (Fisher Scientific 550) at 150 W. The high-energy sonication times ranged from 0.5 to 120 min. The PS solution and MWNT suspension were subsequently mixed (1 wt % MWNTs) in a bath sonicator for 30 min. The mixture was then cast into a culture dish and the toluene allowed to evaporate completely to produce uniform films about 0.4 mm thick. These films were used for *ex situ* mechanical tensile tests on a QT/IL material test system (MTS). Electron transparent MWNT-PS films were made for *in situ* TEM analysis by placing drops of the mixed solution onto Cu TEM grids. As the toluene solvent evaporated, a continuous film was left atop the Cu support. TEM analysis was conducted on a 200 kV JEOL 2000FX LaB<sub>6</sub> TEM.

The optimum sonication time is defined here as the shortest time to disperse MWNTs evenly into the PS matrix, because longer high-energy sonication time has the potential to introduce defects into the MWNTs.<sup>19</sup> Since the nanotube additions caused the PS to become optically opaque, we could evaluate the dispersion homogeneity down to the micron length scale by transmission optical microscopy. TEM was used to assess the homogeneity over smaller length scales. We found that the optimum sonication times increased with the nanotube length, 30 min for 15  $\mu\text{m}$  long tubes and 1 h for 50  $\mu\text{m}$  long tubes. Figure 1 shows a typical TEM image of a composite with nanotubes of 33.6 nm average diameter well dispersed down to the micrometer length scale. The inset in Fig. 1 quantifies the loading of nanotubes over different length scales, and it shows the standard deviation (a measure of the homogeneity) decreases to 0.08 wt % from the average 1 wt % at a length scale of 1.2  $\mu\text{m}$ . The TEM image also reveals that some defects were present in

<sup>a)</sup>Author to whom correspondence should be addressed; electronic mail: ecdickey@engr.uky.edu

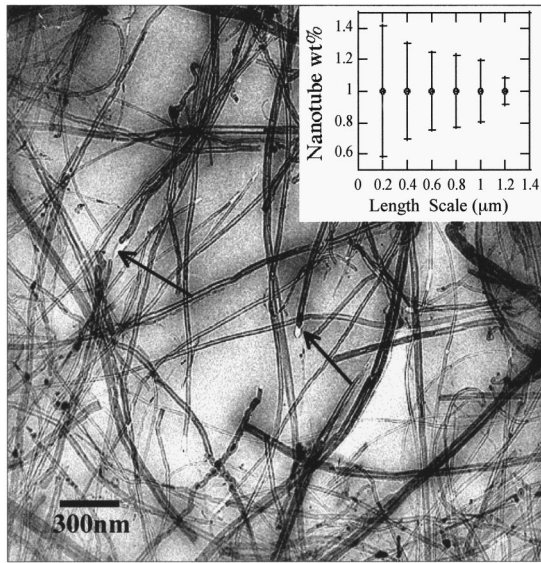


FIG. 1. TEM image of MWNT-PS film in which the nanotubes are homogeneously distributed in the polystyrene matrix at  $\sim 1 \mu\text{m}$  length scale. The inset is the MWNT weight fraction as a function of length scale, which was determined by measuring the weight fraction of nanotubes at areas in the TEM image. The error bars represent the standard deviation of the experimental data, which reflects the homogeneity of the distribution.

the as-prepared samples as a result of polymer shrinkage primarily at the ends of the nanotubes (see arrows in Fig. 1).

Macroscopic tensile tests were performed on the higher (280 000) molecular weight PS which is less brittle in nature than the 48 000 molecular weight PS. Because the less brittle matrix is less sensitive to surface flaws, repeatable tensile tests could be made. Two different types of samples were prepared, one with nanotubes (#1) of  $15 \mu\text{m}$  average length and the other with nanotubes (#2) of  $50 \mu\text{m}$  average length. Both nanotube sets had average diameters of  $\sim 30 \text{ nm}$ . The tensile properties of the MWNT-PS composite films are shown in Table I. Compared with the blank PS, an addition of 1 wt % MWNTs results in about a 25% increase in break stress for both sample types. The elastic modulus increases by 35% and 42% for samples 1 and 2, respectively, indicating a dependence on the average length-to-diameter ratio ( $l/d$ ) of nanotubes. The significance of this  $l/d$  ratio of nanotube will be discussed later.

Ideally, if the reinforcing phase (MWNT) bonds strongly to the matrix (PS), the external tensile load will be transmit-

ted from the matrix to the NTs through the interfacial shear stress. The MWNT-PS composite films can be considered as randomly oriented discontinuous fiber lamina and the composite modulus,  $E_c$ , can be calculated from the following equations.<sup>20</sup>

$$E_c = \left[ \frac{3}{8} \frac{1 + 2(l_{\text{NT}}/d_{\text{NT}})\eta_L V_{\text{NT}}}{1 - \eta_L V_{\text{NT}}} + \frac{5}{8} \frac{1 + 2\eta_T V_{\text{NT}}}{1 - \eta_T V_{\text{NT}}} \right] E_{\text{PS}},$$

$$\eta_L = \frac{(E_{\text{NT}}/E_{\text{PS}}) - 1}{(E_{\text{NT}}/E_{\text{PS}}) + 2(l_{\text{NT}}/d_{\text{NT}})},$$

$$\eta_T = \frac{(E_{\text{NT}}/E_{\text{PS}}) - 1}{(E_{\text{NT}}/E_{\text{PS}}) + 2},$$

where  $E$  represents tensile modulus,  $l_{\text{NT}}$  is the length, and  $d_{\text{NT}}$  is the outer diameter of the nanotubes. The MWNT volume fraction  $V_{\text{NT}}$  was calculated to be 0.487 vol % from the weight fraction (1 wt %), density of MWNT ( $2.16 \text{ g/cm}^3$ ) and PS ( $1.047 \text{ g/cm}^3$ ). The modulus of MWNTs  $E_{\text{NT}}$  is known to be a strong function of NT diameter,<sup>2-4,21,22</sup> and there is also much variability in the reported moduli. For nanotubes similar in diameter to those studied here (30–34 nm), the reported moduli ranges from 0.2 to 0.8 TPa.<sup>2-4,21,22</sup> We have chosen to use the modulus reported in Ref. 22 of 450 GPa since it falls in the mid range of all of the reported moduli and the nanotubes were produced in a similar fashion to those studied here. Substituting these parameters into the previous Eq. (1), we calculated the composite modulus,  $E_c$ , to be  $1.48 E_{\text{PS}}$  for #1 MWNTs and  $1.62 E_{\text{PS}}$  for #2 MWNTs, which are only  $\sim 10\%$  higher than the experimental data of  $1.36 E_{\text{PS}}$  and  $1.42 E_{\text{PS}}$ , respectively. As reflected in Eq. (1), higher length-to-diameter ( $l/d$ ) ratios lead to higher composite moduli. The close agreement, within  $\sim 10\%$ , between the experimental and theoretically predicted composite moduli indicates that the external tensile loads were successfully transmitted to the nanotubes across the NT-PS interface.

To understand the tensile fracture mechanisms of the MWNT-PS composites, we performed complementary deformation studies inside a TEM. Condensing the electron beam onto the MWNT-PS thin film resulted in local thermal stresses which initiated cracks in the composite. The propagation speed of the crack could be controlled by varying the beam flux onto the sample. TEM images were taken at various points along the crack wake to study deformation phenomena in the composite as a function of crack opening

TABLE I. The tensile properties of 1 wt % MWNT-PS composites. The tensile tests were performed under ASTM D882-95a. The moduli were calculated by Eq. (1). Blank PP has a tensile strength of 26 MPa and modulus of 1250 MPa.  $E_M$  is the modulus of pure polymer matrix.

| Composite<br>1 wt % loads | Nanotube or fiber parameters |                                     |                |                  | Composite tensile properties |                                 |                       |            |
|---------------------------|------------------------------|-------------------------------------|----------------|------------------|------------------------------|---------------------------------|-----------------------|------------|
|                           | dia. ( $d$ )<br>(nm)         | length ( $l$ )<br>( $\mu\text{m}$ ) | Ratio<br>$l/d$ | Modulus<br>(MPa) | Strength<br>(MPa)            | Modulus<br>(MPa)                | Calculated<br>modulus | Reference  |
| Blank PS                  | ...                          | ...                                 | ...            | ...              | $12.8 \pm 1$                 | $1190 \pm 130$<br>( $E_M$ )     | ...                   | This study |
| PS+#1 MWNT                | 33.6                         | 15                                  | 446            | 450              | $16 \pm 0.2$                 | $1620 \pm 130$<br>( $1.36E_M$ ) | $1.48E_M$             | This study |
| PS+#2 MWNT                | 30                           | 50                                  | 1167           | 450              | $16 \pm 2$                   | $1690 \pm 130$<br>( $1.42E_M$ ) | $1.62E_M$             | This study |
| PP+VGCF                   | 200                          | 3.6                                 | 18             | 240              | $\sim 28$                    | $\sim 1.0E_M$                   | $1.06E_M$             | 23         |
| PS+ $E-75$ fiber          | 9000                         | 400                                 | 44             | 600              | ...                          | ...                             | $1.14E_M$             | 24         |

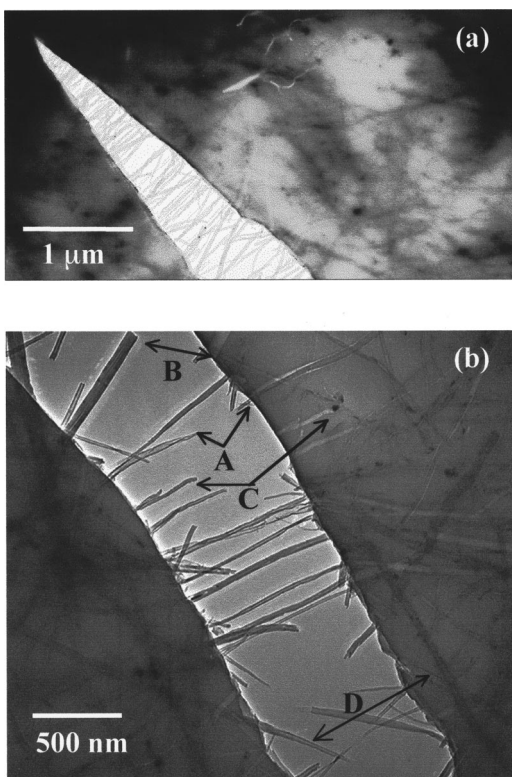


FIG. 2. *In situ* TEM observation of crack nucleation and propagation in MWNT-PS thin films induced by thermal stresses. The cracks propagate along weak NT-PS interfaces or relatively low NT density regions. The MWNTs tend to align and bridge the crack wake then break and/or pull out of the matrix.

displacement. *In situ* TEM observations (Fig. 2) show that the cracks tend to nucleate at low nanotube density areas then propagate along weak NT-PS interfaces or relatively low NT density regions. The NTs align perpendicular to the crack direction and bridge the crack faces in the wake, thus providing closure stresses across the crack faces. When the crack opening displacement exceeds  $\sim 800$  nm, the nanotubes begin to break and/or pull out of the matrix. According to Fig. 2(b), about half of the aligned nanotubes have broken and subsequently pulled out of the matrix [see tube B in Fig. 2(b)]. NTs that are aligned more parallel to the crack propagation direction tend to break between the crack faces rather than in the matrix [see tube D in Fig. 2(b)]. Some tubes have broken at obvious defects, such as tube C in Fig. 2(b), which has broken at the Fe catalyst particle. Annealing the NTs at high temperatures ( $>2200$  °C) can be used to remove the Fe catalyst inclusions and other defects and potentially increase the strength of the NTs and the composites derived from them.

It is important to compare the earlier results to commercial carbon fiber reinforced polymers to assess if the MWNTs are advantageous to existing materials systems. Using Eq. (1) we have computed the composite moduli using parameters for a vapor-grown carbon fiber (VGCF)<sup>23</sup> and a typical commercial high-modulus carbon fiber ( $E=75$ ).<sup>24</sup> The experimental moduli of VGCF-polypropylene (PP) composite with 1 wt % ( $\sim 0.5\%$  vol %) VGCF reported in Ref. 23 is close to the calculated value. For similar loadings, the

MWNTs are superior to the carbon fibers, primarily due to their very large  $l/d$  ratio. According to tensile test results of VGCF-PP composites reported by Tibbet,<sup>23</sup> it is necessary to add 5 vol % ( $\sim 10$  wt %) of VGCF to increase the PP matrix moduli by the same extent observed in 1 wt % MWNT samples. If the  $l/d$  ratios of the carbon fibers were made comparable to the nanotubes, they would have to be several millimeters long which could hamper composite processing. Moreover, because of the large size of the carbon fibers, it would not be possible to achieve the same level of homogeneity over micrometer length scales.

In summary, homogeneous distribution of MWNTs in polystyrene matrices has been achieved by an ultrasonic assisted solution-evaporation method. Addition of only 1 wt % MWNTs to polystyrene increases the polymer mechanical properties significantly. The tensile tests and *in situ* TEM observations show that the external load can be effectively transferred to the nanotubes. Because of their small size and large  $l/d$  ratios, the MWNTs are advantageous to commercially available carbon fibers with similar moduli.

This work was supported by the National Science Foundation MRSEC for Advanced Carbon Materials (DMR-9809686).

- <sup>1</sup>M. S. Dresselhaus, G. Dresselhaus, and P. C. Eklund, *Science of Fullerenes and Carbon Nanotubes* (Academic, New York, 1996), p. 802.
- <sup>2</sup>M. M. J. Treacy, T. W. Ebbesen, and J. M. Gibson, *Nature (London)* **381**, 678 (1996).
- <sup>3</sup>E. W. Wong, P. E. Sheehan, and C. M. Lieber, *Science* **277**, 1971 (1997).
- <sup>4</sup>P. Poncharal, Z. L. Wang, D. Ugarte, and W. A. de Heer, *Science* **283**, 1513 (1999).
- <sup>5</sup>B. I. Yakobson and R. E. Smalley, *Am. Sci.* **85**, 324 (1997).
- <sup>6</sup>J. Sandler, M. S. P. Shaffer, T. Prasse, W. Bauhofer, K. Schulte, and A. H. Windle, *Polymer* **40**, 5967 (1999).
- <sup>7</sup>C. A. Grimes, C. Mungle, D. Kouzoudis, S. Fang, and P. C. Eklund, *Chem. Phys. Lett.* (in press).
- <sup>8</sup>H. Ago, K. Petritsch, M. S. P. Shaffer, A. H. Windle, and R. H. Friend, *Adv. Mater.* **11**, 1281 (1999).
- <sup>9</sup>R. Andrews, D. Jacques, A. M. Rao, F. Derbyshire, D. Qian, X. Fan, E. C. Dickey, and J. Chen, *Chem. Phys. Lett.* **303**, 467 (1999).
- <sup>10</sup>S. B. Sinnott, R. Andrews, D. Qian, A. M. Rao, Z. Mao, E. C. Dickey, and F. Derbyshire, *Chem. Phys. Lett.* **315**, 25 (1999).
- <sup>11</sup>P. M. Ajayan, O. Stephan, C. Colliex, and D. Trauth, *Science* **265**, 1212 (1994).
- <sup>12</sup>L. S. Schadler, S. C. Giannaris, and P. M. Ajayan, *Appl. Phys. Lett.* **73**, 3842 (1998).
- <sup>13</sup>O. Lourie and H. D. Wagner, *Appl. Phys. Lett.* **73**, 3527 (1998).
- <sup>14</sup>O. Lourie, D. M. Cox, and H. D. Wagner, *Phys. Rev. Lett.* **81**, 1638 (1998).
- <sup>15</sup>H. D. Wagner, O. Lourie, Y. Feldman, and R. Tenne, *Appl. Phys. Lett.* **72**, 188 (1998).
- <sup>16</sup>L. Jin, C. Bower, and O. Zhou, *Appl. Phys. Lett.* **73**, 1197 (1998).
- <sup>17</sup>C. Bower, R. Rosen, L. Jin, J. Han, and O. Zhou, *Appl. Phys. Lett.* **74**, 3317 (1999).
- <sup>18</sup>R. Andrews, E. Dickey, D. Qian, B. Knutson, B. Safadi, B. Moore, and F. Derbyshire, *Proceedings of Carbon'99*, Charleston, SC, 1999, p. 258.
- <sup>19</sup>K. L. Lu, R. M. Lago, Y. K. Chen, M. L. H. Green, P. F. Harris, and S. C. Tsang, *Carbon* **34**, 814 (1996).
- <sup>20</sup>P. K. Mallick, *Fiber-reinforced Composites* (Marcel Dekker, New York, 1993), p. 130.
- <sup>21</sup>M. Yu, O. Lourie, M. J. Dyer, K. Moloni, T. F. Kelly, and R. S. Ruoff, *Science* **287**, 637 (2000).
- <sup>22</sup>Z. W. Pan, S. S. Xie, L. Lu, B. H. Chang, L. F. Sun, W. Y. Zhou, G. Wang, and D. L. Zhang, *Appl. Phys. Lett.* **74**, 3152 (1999).
- <sup>23</sup>G. G. Tibbetts and J. J. Mchugh, *J. Mater. Res.* **14**, 2871 (1999).
- <sup>24</sup>D. D. L. Chung, *Carbon Fiber Composites* (Butterworth-Heinemann, Boston, 1994), p. 67.